Imprinting of Chiral Molecular Recognition Sites in Thin TiO_2 Films Associated with Field-Effect Transistors: Novel Functionalized Devices for Chiroselective and Chirospecific Analyses

Michal Lahav, Andrei B. Kharitonov, and Itamar Willner*[a]

Abstract: (*R*)- or (*S*)-2-Methylferrocene carboxylic acids, (*R*)-**1** or (*S*)-**1**, (*R*)- or (*S*)-2-phenylbutanoic acid, (*R*)-**2** or (*S*)-**2**, and (*R*)- or (*S*)-2-propanoic acid, (*R*)-**3** or (*S*)-**3**, can be imprinted in thin TiO_2 films on the gate surface of ion-sensitive field-effect transistor (ISFET) devices. The imprinting is performed by hydrolyzing the respective carboxylate Ti^{IV} butoxide complex on the gate surface, followed by washing off the acid from the resulting TiO_2 film. The imprinted sites reveal chiroselectivity only towards the sensing of the imprinted enantiomer. The chiral recognition sites reveal not only chiroselectivity but also chirospecificity and, for example, the (*R*)-**2**-imprinted film is active in the sensing of (*R*)-**2**, but insensitive towards the sensing of (*R*)-2-phenylpropanoic acid, (*R*)-**3**, which exhibits a similar chirality. Similarly, the (*R*)-**3**-imprinted film is inactive in the analysis of (*R*)-**2**. The chiroselectivity and chirospecificity of the resulting imprinted films are attributed to the need to align and fit the respective substrates in precise molecular contours generated in the cross-linked TiO_2 films upon the imprinting process.

Keywords: field-effect transistor · imprinting · molecular recognition · sensors · titanium oxide

Introduction

Imprinting of molecular recognition sites in bulk polymer or inorganic matrices has been a subject of extensive research efforts in the last two decades.[1, 2] Two general strategies have been suggested to generate the molecular-imprinted recognition sites. One method includes the polymerization of monomer units complementary to the chemical functionalities in the substrate molecule, followed by physical removal of the imprinted substrate by a washing process.[3, 4] The second approach includes the covalent attachment[5] or coordination[6] of the substrate to polymerizable monomer units. Polymerization of the units followed by chemical cleavage of the bonds results in the imprinted molecular recognition sites. Molecular-imprinted inorganic matrices have been prepared by the incorporation of substrates in silica gels[7] or TiO_2[8] followed by the removal of the imprinted substrate from the respective oxides. Inorganic oxides with selective affinities for the imprinted substrate and chiroselective imprinted[9] sites have been reported. The different imprinted matrices have been used for chromatographic separations[10, 11] and for selective reactions in the imprinted cavities.[12] Recently, the effect of chiral cavities on the ligand exchange in platinum complexes was addressed.[13] The use of imprinted molecular recognition sites in membrane assemblies is particularly tempting for selective sensing applications. Although different sensors based on the imprinting process have been reported,[14] the method suffers from basic limitations: 1) The imprinted polymer matrices are usually thick, and the number of recognition sites per unit volume of imprinted matrix is relatively low; this introduces diffusion barriers for the analyte substrate, resulting in slow response-times and moderate sensitivities. 2) It is difficult to electrically contact the molecular recognition sites with electronic transducers, and thus the electronic transduction of the sensing process is problematic. Indeed, most of the sensor devices based on molecular-imprinted membranes are either optical[15] or include the microgravimetric, quartz-crystal-microbalance (QCM) analysis of the substrate.[16] Recently, methods to imprint molecular recognition sites in two-dimensional monolayers assembled on electrodes were reported.[17, 18] The close proximity between the electrode and the binding sites enabled the electrochemical transduction (amperometric or capacitance signals) of the formation of the affinity complexes between the substrate and the imprinted sites. In a preliminary study[19] we reported on the assembly of selective molecular recognition sites for chloro aromatic acids in TiO_2 thin films associated with the gate interface of an ion-sensitive field-effect transistor (ISFET) device. Specific binding sites

[a] Prof. Dr. I. Willner, M. Lahav, Dr. A. B. Kharitonov
Institute of Chemistry, The Hebrew University of Jerusalem
Jerusalem 91904 (Israel)
Fax: 972-2-6527715
E-mail: willnea@vms.huji.ac.il

Supporting information for this article is available on the WWW under http://www.wiley-vch.de/home/chemistry/ or from the author.

0947-6539/01/0718-3992 $ 17.50+.50/0

for 4-chlorophenoxyacetic acid or 2,4-dichlorophenoxyacetic acid in the TiO_2 film were produced. Variation of the gate potential upon the binding of the host substrate, by changing the degree of proton dissociation of the oxide interface, enabled the ISFET-transduction of the sensing processes. Here we wish to report on the imprint of chiral molecular recognition sites in TiO_2 films associated with the gate surface on an ISFET and on the chiroselective and chirospecific sensing of the imprinted substrates.

Results and Discussion

Scheme 1 outlines the method to assemble the imprinted TiO_2 film on the Al_2O_3-gate interface of the ISFET device. The titanium(IV)butoxide–carboxylate complex is polymerized by hydration on the gate interface followed by drying of the resulting TiO_2 film. The resulting TiO_2 film is washed with an ammonia solution to exclude the carboxylate units and to generate the structural contours for the association of the imprinted substrate. The hydrolysis of the carboxylate generates surface Ti-OH groups that control the gate potential. The secondary binding of the carboxylate analyte removes part of the hydroxyl functionalities [Eq. (1)], and the gate potential is altered, thus enabling the electronic transduction of the association of the substrate to the imprinted sites in the membrane film by the ISFET device.

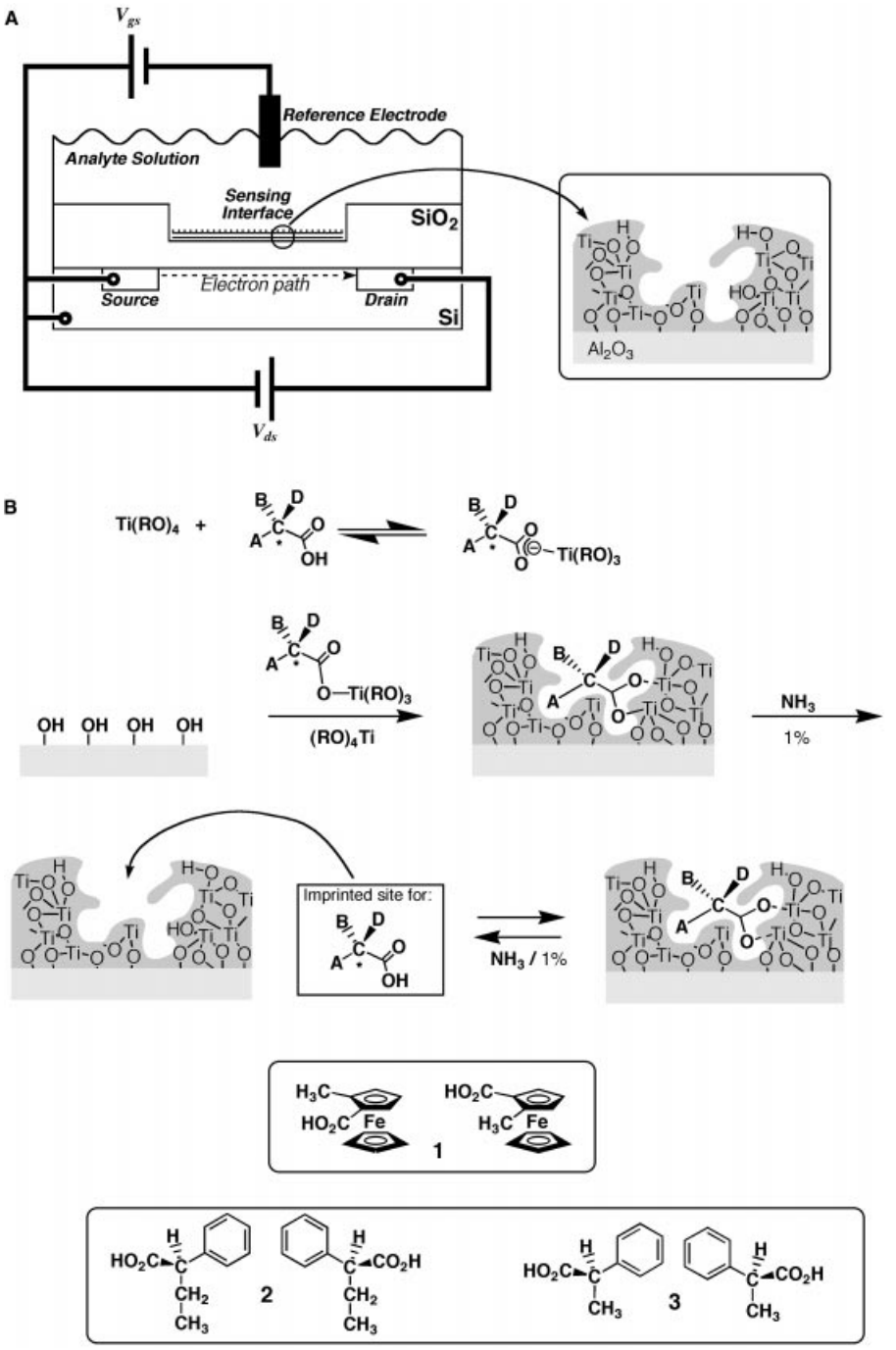

Scheme 1. A) Schematic configuration of the molecular imprinted ISFET device. B) Preparation of molecular imprinted sites for carboxylic acids in a TiO_2 film acting as the sensing interface on the ISFET gate.

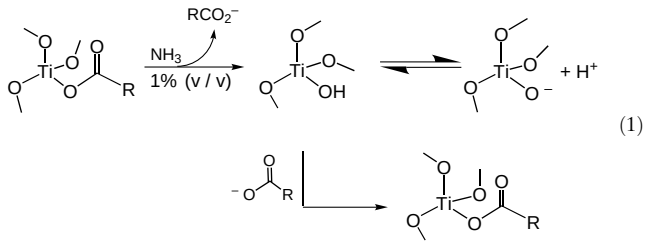

(1)

The first pair of chiral substrates that were examined by this method were (*S*)-2-methylferrocene carboxylic acid and (*R*)-2-methylferrocene carboxylic acid, (*S*)-**1** and (*R*)-**1**, respectively. The two chiral substrates were imprinted in the respective TiO_2-functionalized ISFETs. Figure 1A shows the responses of the (*S*)-**1**-imprinted ISFET device upon sensing different concentrations of (*S*)-**1**, curve a, and upon an attempt to sense (*R*)-**1** by the device, curve b. It is clear that the system reveals chiroselectivity, and the device responses to the imprinted substrate. The device is, however, insensitive to the (*R*)-**1** enantiomer. The system is able to sense (*S*)-**1** in

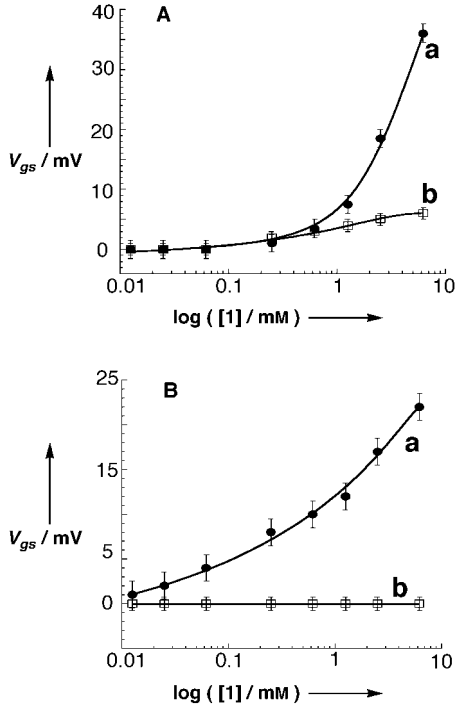

Figure 1. A) The gate-source voltage (V_{gs}) of the (*S*)-**1**-imprinted TiO_2-film-functionalized ISFET device upon: a) interaction with variable concentrations of (*S*)-**1** and b) treatment with variable concentrations of (*R*)-**1**. B) The gate-source voltage of the (*R*)-**1**-imprinted TiO_2-film-functionalized ISFET device upon: a) interaction with variable concentrations of (*R*)-**1** and b) treatment with variable concentrations of (*S*)-**1**.

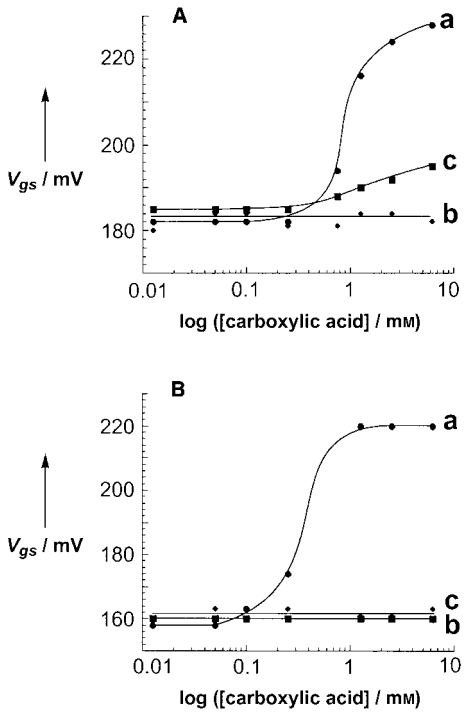

Figure 2. A) The gate-source voltage (V_{gs}) of the (*S*)-**2**-imprinted TiO_2-film-functionalized ISFET device upon: a) interaction with variable concentrations of (*S*)-**2**, b) treatment with different concentrations of (*R*)-**2**, and c) treatment with different concentrations of (*S*)-**3**. B) The gate-source voltage (V_{gs}) of the (*R*)-**2**-imprinted TiO_2-film-functionalized ISFET-device upon: a) interaction with variable concentrations of (*R*)-**2**, b) treatment with different concentrations of (*S*)-**2**, and c) treatment with variable concentrations of (*R*)-**3**.

the concentration range of 0.125 to 6.25 mM with a lower detection limit for the analysis of (*S*)-**1** that corresponds to 0.6 mM, and an average sensitivity of 16 ± 1 mV dec^{-1}. Figure 1B shows the "mirror experiment" in which the TiO_2 film associated with the gate of the ISFET is imprinted with the (*R*)-**1** enantiomer, and the response of the system to (*R*)-**1**, curve a or (*S*)-**1**, curve b, are examined. The system reveals complete chiroselectivity for the imprinted substrate. While (*R*)-**1** is effectively sensed in the concentration range of 0.05 to 6.25 mM with a lower detection limit of 0.10 mM and an average sensitivity that corresponds to 18 ± 1 mV dec^{-1}, the (*S*)-**1** enantiomer is not recognized by the membrane and no response of the system is detected.[20] The system reveals full reversibility and the associated substrate can be washed off from the membrane (with 1% NH_3 solution), a process that regenerates the sensing membrane. The functionalized ISFET device exhibits stability towards the chiroselective analysis of the chiral ferrocene derivatives for at least one week.

The chiroselectivity of the imprinted ISFET devices is even more impressive upon imprinting the enantiomers of 2-phenyl alkanoic acids in the TiO_2 films and the analysis of the respective acids by the ISFET devices. (*R*) or (*S*)-2-phenylbutanoic acid, (*R*)-**2** and (*S*)-**2**, were imprinted in the TiO_2 films. Figure 2A shows the results corresponding to the analysis of the enantiomers by the (*S*)-**2**-imprinted membrane ISFET device. The imprinted substrate, (*S*)-**2**, is effectively sensed by the device, curve a, in the narrow concentration range of 0.25 to 2.5 mM with the lower detection limit corresponding to 0.50 mM. The (*S*)-**2** imprinted membrane is, however, insensitive to the (*R*)-**2** substrate, and no signal is transduced by the ISFET device within the entire concentration range in which (*S*)-**2** is detected, Figure 2A, curve b. Interestingly, the (*S*)-**2**-imprinted TiO_2 membrane reveals only a minute affinity for (*S*)-2-phenylpropanoic acid, (*S*)-**3**, (the slope of the calibration curve corresponds to 5 ± 0.5 mV dec^{-1} in the concentration range of 0.4 to 6.25 mM), Figure 2A, curve c. That is, even though (*S*)-**2** and (*S*)-**3** exhibit a similar configurational stereochemistry, shortening of the alkane chain by a single methylene unit yields almost complete structural differentiation by the sensing film. This stereochemical specificity of the imprinted TiO_2 film is attributed to a cooperative binding effect of the imprinted molecular contour and the carboxylic acid ligation site upon the association of the imprinted substrate to the cross-linked Ti-O-Ti matrix. For effective binding of the chiral carboxylic acid (*S*)-**2** to the Ti-OH center, the association of the substrate to the imprinted molecular contour through the terminal methyl group of the four-carbon chain is essential in order to gain the appropriate structural orientation of the substrate. Similar behavior is observed upon analyzing the two enantiomers with the (*R*)-**2**-imprinted membrane, Figure 2B. The imprinted membrane effectively binds (*R*)-**2**, curve a, in the concentration range of 0.0625 to 1.25 mM, with an average slope of the calibration curve that corresponds to 42 ± 2 mV dec^{-1} and with a lower detection limit of 0.08 mM.[20] The imprinted membrane is insensitive to the (*S*)-**2** enan-

0947-6539/01/0718-3994 $ 17.50+.50/0 *Chem. Eur. J.* **2001**, *7*, No. 18

tiomer, Figure 2B, curve b. As stated above, the enantiomer (*R*)-**3**, which exhibits identical stereochemistry to the imprinted substrate but includes an alkyl chain shorter by a single methylene group, is not detected by the functionalized ISFET, Figure 2B, curve c. That is, the imprinted ISFET devices reveal not only chiroselectivity leading to complete differentiation between the imprinted (*R*) and (*S*) substrates, but also impressive chirospecificity that enables the selective recognition of the two structural analogues (*R*)-**2**, (*R*)-**3** and (*S*)-**2**, (*S*)-**3**.

The opposite imprinting procedure in which the enantiomers of **3** are imprinted in the TiO_2 film, leads similarly to the chiroselective and chirospecific membrane-functionalized ISFET devices. Figure 3A exemplifies the performance of

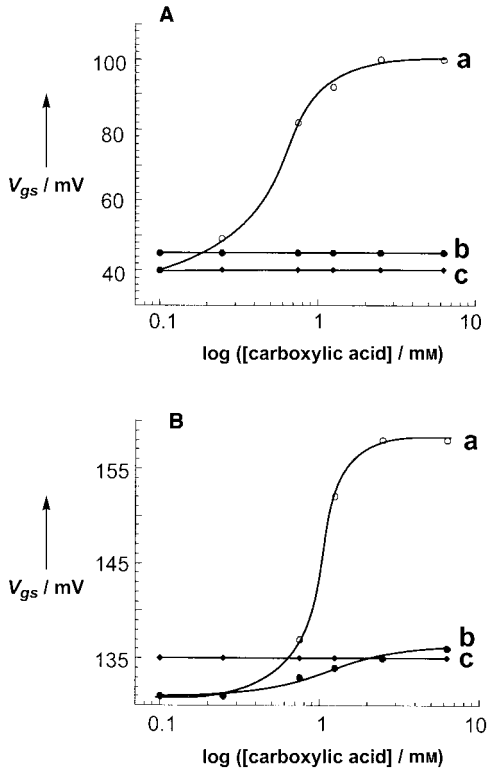

Figure 3. A) The gate-source voltage (V_{gs}) of the (*R*)-**3**-imprinted TiO_2-film-functionalized ISFET device upon: a) interaction with variable concentrations of (*R*)-**3**, b) treatment with different concentrations of (*S*)-**3**, and c) treatment with variable concentrations of (*R*)-**2**. B) The gate-source voltage of the (*S*)-**3**-imprinted TiO_2-film-functionalized ISFET device upon: a) interaction with variable concentrations of (*S*)-**3**, b) treatment with different concentrations of (*R*)-**3**, and c) treatment with variable concentrations of (*S*)-**2**.

the (*R*)-**3**-imprinted membrane. The imprinted substrate (*R*)-**3** is effectively sensed by the device in the concentration range of 0.05 to 1.25 mM with the detection limit of 0.10 mM and an average sensitivity that corresponds to 55 ± 2 mV dec^{-1}, Figure 3A, curve a. The (*R*)-**3**-imprinted membrane is inactive in sensing the enantiomer (*S*)-**3**, Figure 3A, curve b. Similarly, the (*R*)-**3**-imprinted film is insensitive for the analysis of (*R*)-**2**, which exhibits a chirality similar to that of (*R*)-**3**, Figure 3A, curve c. Thus the imprinted matrix is able to distinguish between two substrates that differ only by a single CH_2 group. The specificity of the imprinted TiO_2 film for (*R*)-**3** is attributed to the cross-linked matrix of the interface. That is, the generated molecular contour for (*R*)-**3** cannot spatially accommodate the larger substrate (*R*)-**2**. Analogous results are observed upon interaction of the (*S*)-**3**-imprinted ISFET device with the two enantiomers (*S*)-**3** and (*R*)-**3**, Figure 3B. The imprinted substrate (*S*)-**3** is effectively sensed by the interface in the concentration range of 0.3 – 1.25 mM with the lower detection limit of 0.45 mM. The average slope of the calibration plot corresponds to 35 ± 2 mV dec^{-1}, Figure 3B, curve a. The (*S*)-**3**-imprinted membrane is, however, almost insensitive to the (*R*)-**3** enantiomer, revealing a minute sensitivity of 4 ± 0.3 mV dec^{-1} in the range of 0.6 – 6.25 mM, which is within the error of measurement, Figure 3B, curve b. Similarly, the (*S*)-**3**-imprinted film is insensitive towards the sensing of (*S*)-**2**, which exhibits a chirality identical to that of (*S*)-**3**, Figure 3B, curve c. These results clearly indicate that the membrane is an active sensing interface for the imprinted chiral substrate. The imprinted membrane can distinguish enantiomers of similar chirality that differ by a single methylene unit. Thus, the imprinted interface reveals chiroselectivity and chirospecificity.

An attempt was made to characterize the sensing interface and the imprinted sites in the film. The film thickness was determined by the use of impedance spectroscopy measurements on the modified gate interface.[21] The impedance features of the gate interface are controlled by the chemical composition of the modified gate.[22, 23] In a recent study we suggested the use of impedance spectroscopy measurements on a functionalized gate as a method to evaluate the thickness of chemically-assembled thin films on the gate surface.[24] According to this method, the transconductance functions of the system are recorded at variable applied frequencies, and the time constants τ_1 [Eq. (2)] and τ_2 [Eq. (3)] are extracted

$$\tau_1 = R_{mem}(C_{mem} + C_{ox}) \approx R_{mem} C_{ox} \quad (2)$$

$$\tau_2 = R_{mem} C_{mem} \quad (3)$$

$$C_{mem} = \frac{\varepsilon_o \varepsilon_{mem} A}{\delta_{mem}} \quad (4)$$

from the curves, see Figure 4. By using the time constants, the resistance of the TiO_2 film membrane (R_{mem}) and the capacitance of the TiO_2 film (C_{mem}) can be determined. The value C_{ox} corresponds to the capacitance of the Al_2O_3

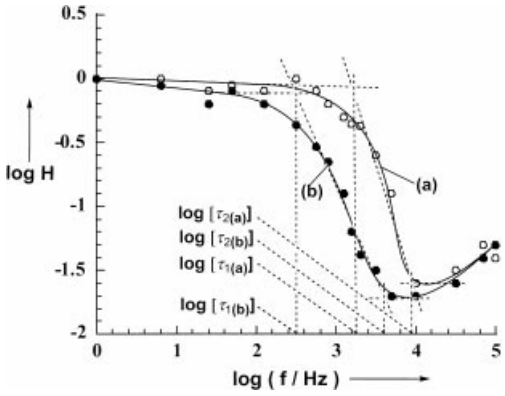

Figure 4. Transconductance curves of: a) the bare ISFET device and b) the (*R*)-**3**-imprinted TiO_2-film-functionalized ISFET device.

interface on which the TiO_2 film is assembled. From these values, the film thickness δ_{mem} can be determined by using Equation (4), in which ε_o and ε_{mem} are the dielectric constants of the vacuum ($\varepsilon_o = 8.85 \times 10^{-12}\,F\,m^{-1}$) and the dielectric constant of the membrane, respectively, and A is the gate area.

Figure 4 shows the transconductance curves at variable frequencies corresponding to the bare ISFET device, curve a, and the TiO_2 film-functionalized gate, curve b. Using the derived C_{mem} and $\varepsilon_{mem} \approx 10$, we estimate the TiO_2 film thickness to be 85 ± 10 μm.

To further characterize the sensing interface associated with the gate, we attempted to estimate the number of imprinted sites in the sensing membrane. Towards this goal we imprinted $^{14}CH_3CO_2H$ in the TiO_2 membrane associated with the ISFET device, by a similar procedure outlined for the different acids. We measured the radioactive counts of the resulting film and the radioactive counts resulting in the solution upon washing the imprinted film with 1 % NH_3. We find that about 65 – 70 % of the radioactive counts associated with the film are washed off. Using these data, we estimate that approximately 3.68×10^{18} imprinted sites per gram are associated with the TiO_2 sensing interface.[25] It should be noted that since the radioactive label is acetic acid, the number of imprinted recognition sites in the sensing interface may be considered only as a rough estimate of the number of recognition sensing sites of the other acids described in this study.

Conclusions

The present study has revealed the imprint of chirospecific and chiroselective molecular recognition sites in TiO_2 thin-films associated with a field-effect transistor. The functionalized ISFET device provides a sensitive electronic transducer for the detection of the affinity interaction between the imprinted substrate and the recognition site. The interesting observation is that not only the different imprinted enantiomers yield chiroselective recognition sites for the respective enantiomers, but yield chirospecific sites that differentiate structurally related compounds of similar chirality. For example, this was clearly demonstrated by the fact that the (*R*)-**2**-imprinted membrane is insensitive for sensing (*R*)-**3**, and, similarly, the (*R*)-**3** imprinted TiO_2 film is inactive in the binding of (*R*)-**2**. This unique chirospecificity was attributed to the need for precise fitting and alignment of the imprinted substrate in the imprinted molecular contour with respect to the Ti-OH carboxylate ligating site.

Our study has also revealed an effort to characterize the imprinted sensing interface on the gate surface of the ISFET, by the combination of impedance measurements and radioactive labeling experiments. The impedance measurements[22] provide a sensitive technique to characterize the structure of chemically assembled dielectric membrane films on the gate surface of ISFETs.

Experimental Section

Materials: (*S*)- and (*R*)-2-methylferrocene carboxylic acids, (*S*)-**1** or (*R*)-**1**, respectively, were synthesized according to literature.[26] (*S*) or (*R*)-2-phenylpropanoic acid, (*S*)-**2** and (*R*)-**2**, respectively, and (*S*) or (*R*)-2-phenylbutanoic acid, (*R*)-**3** and (*S*)-**3**, respectively, were purchased from Sigma. Ti^{IV} butoxide was purchased from Aldrich. All other chemicals (Sigma or Aldrich) were of analytical grade and used as received. Ultrapure water from Seralpur PRO 90 CN was used throughout all the experiment.

ISFET preparation: A solution of Ti^{IV} butoxide in ethanol/toluene (1:1) was treated with the respective carboxylic acid. The resulting mixture, which included the Ti^{IV}-butoxide – carboxylate complex, was deposited onto the gate surface. The modification of the Al_2O_3-gate of the ISFET device was performed by placing a 0.4 μL drop of the Ti^{IV}-butoxide – carboxylate complex solution on the gate interface. The system was then dried in an oven (Eurotherm) at 40 °C overnight. The resulting modified chip was thoroughly rinsed with toluene and then with the working buffer solution. The sol-gel polymerization of the mixture on the alumina oxide gate interface resulted in a thin TiO_2 film with the embedded carboxylate. Treatment of the film with ammonia solution (1 % v/v for 2 min) led to the elimination of the carboxylate and the formation of imprinted molecular sites for the respective acid within the TiO_2 film.

Measurements: Al_2O_3-gate (20×700 μm^2) ion-sensitive field-effect transistors (IMT, Neûchatel, Switzerland) were used. An Ag/AgCl electrode was used as a reference electrode. The chip modified by the molecular-imprinted TiO_2 thin film was immersed in the analysis cell that included phosphate buffer solution (0.8 mL, 0.1 M, pH 7.2) and the respective acid at different concentrations. The output signal between the ISFET source and the reference electrode was recorded by using a semiconductor parameter analyzer (HP 4155B). Each measurement was performed for 15 minutes with a time interval of 2 minutes. The configuration of the system enabled the measurement of the source-gate voltage (V_{gs}), while the drain current (I_d) and the source-drain voltage (V_{ds}) remained constant ($I_d = 100$ μA and $V_{ds} = 1.5$ V). The difference in the V_{gs} potentials for the ISFET modified by the TiO_2 films with and without the embedded carboxylic acid residue was plotted. The experiments were carried out at ambient temperature without any stirring in order to simulate real conditions of possible future in vivo applications. Reproducibility of the measurements was ± 2 mV in a number of experiments ($n = 5$). All the measurements were performed using a phosphate buffer solution (0.1 M, pH 7.2).

Evaluation of TiO_2 film thickness: The TiO_2 film thickness was determined by the use of impedance spectroscopy measurements on the ISFET device.[21] The electronic circuit (see Supporting Information) was used to follow the impedance properties of the modified ISFET device. This circuit was recently used to characterize the modification of the gate interface with different thin films.[24] The functionalized Al_2O_3-gate ISFET devices and a Pt wire ($D = 0.8$ mm), acting as a counter electrode and positioned 2 mm from the gate interface, were immersed in the cell filled with 0.8 mL of the analyzed solution. The ISFET characteristic curves (I_d vs V_{ds} for the appropriate V_{gs} values) were recorded with a HP 4155B semiconductor parameter analyzer. The measurement setup consisted of a programmable electrometer (Keithley 617), a lock-in amplifier (Stanford Research System, Model SR 830 DSP), and a two-channel digital real-time oscilloscope (Tektronix TDS 220). For the impedance spectroscopy measurements, the ISFET was conjugated to the electronic circuit. The V_{ds} value was adjusted to 1.5 V as indicated on a SKL MAS930L multimeter by using a potentiometer. Then, the Keithley voltage source was adjusted to provide a DC bias potential of 0.75 V, and the I_d value, which corresponded to 100 μA, was adjusted by using the same multimeter. These operating conditions of the ISFET enabled us to obtain an undistorted operational amplifier output, detected on the Tektronix oscilloscope, when an AC voltage of 0.3 V RMS was applied from the internal sine wave reference of the lock-in amplifier. To determine the transconductance transfer functions, the output potential, V_{out}, at variable frequencies from 1 Hz to 100 kHz, was related to the imaginary impedance, Z_{im}. The values of the output potentials corresponding to Z_{im} were normalized at 1 Hz to give the respective transfer function.[24]

Radioactive labeling experiments: The procedure for the radioactive labeling experiments was carried out in the same way as described above in part "*ISFET preparation*", in which [2-^{14}C] acetic acid (25 mM) was used as a template molecule. The radioactivity of [2-^{14}C] acetic acid embedded in the TiO_2 film and in solution was measured by a scintillation counter LS-2800 (Beckman) with 1 % counting accuracy.[19]

0947-6539/01/0718-3996 $ 17.50+.50/0 *Chem. Eur. J.* **2001**, *7*, No. 18

Acknowledgements

This research is supported by The Israel Ministry of Science as an Infrastructure project on Material Science. I.W. acknowledges The Max Planck Research Award for International Cooperation. M.L. acknowledges the support of The Clore Israel Foundation Scholars Programme.

[1] a) K. Haupt, K. Mosbach, *Chem. Rev.* **2000**, *100*, 2495–2504; b) B. Sellergren, *Trends Anal. Chem.* **1997**, *16*, 310–320; c) K. J. Shea, *Trends Polym. Sci. 2* **1994**, 166–173; d) G. Wulff, *Angew. Chem.* **1995**, *107*, 1958–1979; *Angew. Chem. Int. Ed. Engl.* **1995**, *34*, 1812–1832.

[2] a) O. Ramström, R. J. Ansell, *Chirality* **1998**, *10*, 195–209; b) P. A. Brady, J. K. M. Sanders, *Chem. Soc. Rev.* **1997**, *26*, 327–336; c) K. Mosbach, *Trends Biochem. Sci.* **1994**, *19*, 9–14; d) G. Wulff in *Polymeric Reagents and Catalysis* (Ed.: W. T. Ford), American Chemical Society, Washington DC, **1986**, pp. 186–230.

[3] a) K. Mosbach. O. Ramström, *Bio/Technology* **1996**, *14*, 163–170; b) J. U. Klein, M. J. Whitcombe, F. Mulholland, E. N. Vulfson, *Angew. Chem.* **1999**, *111*, 2100–2103; *Angew. Chem. Int. Ed.* **1999**, *38*, 2057–2060.

[4] a) B. Sellergren, K. J. Shea, *J. Chromatogr.* **1993**, *635*, 31–49; b) D. J. O'Shannessy, B. Ekberg, K. Mosbach, *Anal. Biochem.* **1989**, *177*, 144–149; c) B. Sellergren, M. Lepistö, K. Mosbach, *J. Am. Chem. Soc.* **1988**, *110*, 5853–5860.

[5] a) G. Wulff, A. Sarhan, K. Zabrocki, *Tetrahedron Lett.* **1973**, 4329–4332; b) G. Wulff, H.-G. Poll, *Macromol. Chem.* **1987**, *188*, 741–748.

[6] a) K. J. Shea, D. Y. Sasaki, *J. Am. Chem. Soc.* **1991**, *113*, 4109–4120; b) K. J. Shea, D. Y. Sasaki, *J. Am. Chem. Soc.* **1989**, *111*, 3442–3444.

[7] a) K. Sakata, T. Kunitake, *Chem. Lett.* **1989**, 2159–2162; b) A. H. Beckett, P. Anderson, *Nature* **1957**, *179*, 1074–1075.

[8] a) S. W. Lee, I. Ichinose, T. Kunitake, *Langmuir* **1998**, *14*, 2857–2863; b) I. Ichinose, H. Senzu, T. Kunitake, *Chem. Mater.* **1997**, *9*, 1296–1298; c) R. Makote, M. M. Collinson, *Chem. Mater.* **1998**, *10*, 2440–2445.

[9] S. W. Lee, I. Ichinose, T. Kunitake, *Chem. Lett.* **1998**, 1193–1194.

[10] a) B. Sellergren, *J. Chromatogr. A* **1994**, *673*, 133–141; b) L. Schweitz, L. I. Andersson, S. Nilsson, *Anal. Chem.* **1997**, *69*, 1179–1183; c) S. Nilsson, L. Schweitz, M. Petersson, *Electrophoresis* **1997**, *18*, 884–890.

[11] a) O. Brüggemann, R. Freitag, M. J. Whitcombe, E. N. Vulfson, *J. Chromatogr. A* **1997**, *781*, 43–53; b) J. Matsui, Y. Miyoshi, R. Matsui, T. Takeuchi, *Anal. Sci.* **1995**, *11*, 1017–1019; c) B. Sellergren in *A Practical Approach to Chiral Separation by Liquid Chromagoraphy* (Ed. G. Subramanian), VCH, Weinheim **1994**, pp. 69–93; d) O. Brüggemann, K. Haupt, L. Ye, E. Yilmaz, K. Mosbach, *J. Chromatogr. A* **2000**, *889*, 15–24.

[12] a) K. J. Shea, E. A. Thompson, *J. Org. Chem.* **1978**, *43*, 4253–4255; b) J. Damen, D. C. Neckers, *Tetrahedron Lett.* **1980**, *21*, 1913–1916; c) G. Wulff, J. Vietmeier, *Makromol. Chem.* **1989**, *190*, 1727–1735; d) G. Wulff, J. Vietmeier, *Makromol. Chem.* **1989**, *190*, 1717–1726; e) S. E. Byström, A. Borje, B. Akermark, *J. Am. Chem. Soc.* **1993**, *115*, 2081–2083; f) J. V. Beach, K. J. Shea, *J. Am. Chem. Soc.* **1994**, *116*, 379–380.

[13] N. M. Brunkan, M. R. Gagné, *J. Am. Chem. Soc.* **2000**, *122*, 6217–6225.

[14] a) D. Kriz, M. Kempe, K. Mosbach, *Sens. Actuators B* **1996**, *33*, 178–181; b) S. A. Piletsky, E. V. Piletskaya, T. L. Panasyuk, A. V. El'skaya, R. Levi, I. Karube, G. Wulff, *Macromolecules* **1998**, *31*, 2137–2140; c) T. L. Panasyuk, V. M. Mirsky, S. A. Piletsky, O. S. Wolfbeis, *Anal. Chem.* **1999**, *71*, 4609–4613; d) E. Hedborg, F. Winquist, I. Lundström, L. I. Andersson, K. Mosbach, *Sens. Actuators A* **1993**, *36–38*, 796–799.

[15] a) W. Wang, S. H. Gao, B. Wang, *Org. Lett.* **1999**, *1*, 1209–1212; b) Y. Liao, W. Wang, B. Wang, *Bioorg. Chem.* **1999**, *27*, 463–476.

[16] a) C. Malitesta, I. Losito, P. G. Zambonin, *Anal. Chem.* **1999**, *71*, 1366–1370; b) C. D. Liang, H. Peng, X. Y. Bao, L. H. Nie, S. Z. Yao, *Analyst* **1999**, *124*, 1781–1785; c) K. Haupt, K. Noworyta, W. Kutner, *Anal. Commun.* **1999**, *36*, 391–393; d) H. S. Ji, S. McNiven, K. Ikebukuro, I. Karube, *Anal. Chim. Acta* **1999**, *390*, 93–100.

[17] M. Lahav, E. Katz, A. Doron, F. Patolsky, I. Willner, *J. Am. Chem. Soc.* **1999**, *121*, 862–863.

[18] V. M. Mirsky, T. Hirsch, S. A. Piletsky, O. S. Wolfbeis, *Angew. Chem.* **1999**, *111*, 1179–1181; *Angew. Chem. Int. Ed.* **1999**, *38*, 1108–1110.

[19] M. Lahav, A. B. Kharitonov, O. Katz, T. Kunitake, I. Willner, *Anal. Chem.* **2001**, *73*, 720–723.

[20] It should be noted that theoretically the V_{gs} values, the detection regions, and the sensitivity values of the *R*- or *S*-imprinted substrates to the respective *R* or *S* substrates should be identical. The observed differences are attributed to experimental variations in the quality of the generated membranes.

[21] a) A. Friebe, F. Lisdat, W. Moritz, *Sens. Mater.* **1993**, *5*, 65–82; b) M. M. G. Antonisse, B. H. M. Snellink-Ruel R. J. W. Lugtenberg, J. F. J. Engbersen, A. van den Berg, D. N. Reinhoudt, *Anal. Chem.* **2000**, *72*, 343–348.

[22] a) A. Demoz, E. M. J. Verpoorte, D. J. Harrison, *J. Electroanal. Chem.* **1995**, *389*, 71–78; b) R. D. Armstrong, G. Horvai, *Electrochim. Acta* **1990**, *35*, 1–7; c) R. J. W. Lugtenberg, R. J. M. Egberink, A. van den Berg, J. F. J. Engbersen, D. N. Reinhoudt, *J. Electroanal. Chem.* **1998**, *452*, 69–86.

[23] a) E. Souteyrand, J. P. Cloarec, J. R. Martin, C. Wilson, I. Lawrence, S. Mikkelsen, M. F. Lawrence, *J. Phys. Chem. B* **1997**, *101*, 2980–2985; b) M. Maupas, C. Saby, C. Martelet, N. Jaffrezic-Renault, A. P. Soldatkin, M. M. Charles, T. Delair, B. Mandrand, *J. Electroanal. Chem.* **1996**, *406*, 53–58.

[24] A. B. Kharitonov, J. Wasserman, E. Katz, I. Willner, *J. Phys. Chem. B*, **2001**, *105*, 4205–4213.

[25] It should be noted that deposition of the TiO_2 film results in its association onto the gate surface as well as on the ISFET edges that are not active in the sensing process. In order to estimate the net mass of TiO_2 film that is active in the sensing process we determined the total mass of the TiO_2 film generated by the reactant solution using microgravimetric quartz crystal microbalance measurement. Using the film thickness of 85 μm and the area of the gate of $20 \times 700\ \mu m^2$, we estimated the sensing-active TiO_2 weight.

[26] A. D. Ryabov, Y. N. Firsova, V. N. Goral, E. S. Ryabova, A. N. Shevelkova, L. L. Troitskaya, T. V. Demeschik, V. I. Sokolov, *Chem. Eur. J.* **1998**, *4*, 806–813.

Received: February, 2001 [F3089]